

Thermal Convection, Morphological Stability and the Dendritic Growth of Crystals

Kee-Kahb Koo, Ramagopal Ananth, and William N. Gill

Dept. of Chemical Engineering, Rensselaer Polytechnic Institute, Troy, NY 12180

New data on the dendritic growth and microstructure of ice crystals in quiescent pure water are reported for small subcoolings of $0.035\text{ K} < \Delta T < 1.000\text{ K}$, where thermal or natural convection is prevalent. Accurate and systematic measurements of the growth velocity V_G and the tip radii of the edge and basal planes R_1 and R_2 were made as functions of time.

The central point of this work is that with the harmonic mean of the tip radii R_m as the lengthscale, the intensity of natural convection can be correlated accurately by using the thermal convection analogy, $Gr = Re^2$. On this basis, natural convection has a crucial effect on dendritic growth of ice at $\Delta T < 0.35\text{ K}$, the region of subcooling in which the tip of the dendrite splits consistently.

The experiments show that the morphological stability parameter σ^ is independent of subcooling and equals 0.075, when the lengthscale is R_m . With the observed values of R_1 and R_2 , the aspect ratio is 28, and the growth velocity for small ΔT is significantly higher than that predicted by the conduction theory of Horvay and Cahn (1961). Thus, the effect of convection on the growth of ice crystals is more important as the subcooling decreases.*

Moving boundary solutions of the three-dimensional Navier-Stokes and energy equations for the dendritic growth of an elliptical paraboloid were obtained here with the Stokes flow approximation. Experimental observations of the quantities, V_G , R_1 , and R_2 , agree well with predictions of this theory when $Gr = Re_m^2$ is based on R_m . In contrast, if convection is neglected in the theory, it does not agree with the experiments and the difference increases significantly as the subcooling is decreased.

Introduction

The growth of crystals from pure subcooled melts produces dendritic structures. The main characteristic of this tree-like growth is that the leading tip of the main stem propagates in the preferred crystallographic direction. The morphological stability and growth kinetics of the leading tip of an ice dendrite are governed by the solid/liquid interfacial tension, attachment kinetics and transport of latent heat by conduction and convection in the melt. Here we study the growth kinetics and determine the interfacial stability of ice dendrites by conducting

precise experiments at subcoolings as low as 0.035 K , where thermal convection in the melt due to gravity is significant.

Thermal convection is prevalent at low subcoolings. The temperature gradient in the melt causes a density gradient that induces flow in the melt under the influence of gravity. Experiments by Huang and Glicksman (1981) show that the growth rate of succinonitrile dendrites depend on their orientation with respect to gravity. Recently, dendritic growth experiments in space have been proposed by Glicksman et al. (1988) to eliminate gravity-driven convection in the melt. We will show here that the dendritic growth of ice is also affected significantly by natural convection.

Kallungal and Barduhn (1977) investigated the free growth

Correspondence concerning this article should be addressed to W. N. Gill.
The present address of R. Ananth is ARCO Chemical Co., Newtown Square, PA 19073.

of single ice crystals in water with subcoolings ranging from 0.1 to 1 K. They found that the growth rate depended on the orientation of the crystals with respect to the earth. Furthermore, when the crystals grew vertically downward, no steady state was observed due to natural convection as indicated in the photographs reported by Gill (1989). Their forced convection data were correlated well by Kind et al. (1987) on the basis of results obtained for an elliptical paraboloid using the Oseen rectilinear approximation. Fujioka (1978) studied the growth of ice crystals in the region of subcooling of 0.08 K < ΔT < 5.1 K and found that an ice disk sometimes was formed at ΔT < 0.17 K, and dendrites were formed at ΔT > 0.2 K. Chang (1985) measured the growth velocity and tip radius of the basal plane of ice crystals growing in both quiescent and flowing systems. Tirmizi and Gill (1987, 1989) observed ice dendrites growing upward in quiescent pure water and found that natural convection affects significantly the growth velocity and the overall morphology. All of these experiments showed that the shape of the tip of ice dendrites is very close to an elliptical paraboloid and that thermal convection plays a significant role during dendritic growth. As shown in Table 1, however, data on the kinetics of ice dendrites growing in quiescent water are not consistent among the various investigators.

Even though numerous experiments on ice crystal growth have been reported to date, there has been very limited success in reconciling the experimental results with the theory. Ivantsov (1947) was the first to find an exact solution to the diffusion equation for heat transport from a moving solid/liquid interface with a parabolic shape, which resembles the tip of a succinonitrile dendrite. Unlike succinonitrile, ice dendrites are unsymmetrical due to anisotropy in molecular attachment kinetics. Therefore, the transport of heat into the melt is fully three-dimensional and this must be considered in the theory. Horvay and Cahn (1961) extended the solution of Ivantsov to an elliptical paraboloid which is similar to the shape of the ice dendrites. They showed that the aspect ratio, A , has a large effect on the growth kinetics of the dendrites at small subcoolings, and the dimensionless subcooling, St , is related to the aspect ratio, A , and growth Peclet number, $P_G = V_G R_1 / \alpha$, by:

$$St = A^{1/2} \left(\frac{P_G}{2} \right) \exp \left(\frac{P_G}{2} \right) \int_{P_G/2}^{\infty} \frac{e^{-u}}{\left\{ u + (A-1) \left(\frac{P_G}{2} \right) \right\}^{1/2}} du, \quad (1)$$

if one neglects convection in the melt.

In Eq. 1, $A = 1$ represents a paraboloid of revolution; $A = \infty$ is a parabolic cylinder; and $u = P_G/2$ indicates the solid/liquid interface. Dash and Gill (1984) appeared to have been the first to show that if one uses the Oseen approximation of the Navier-Stokes equations, an exact solution can be obtained for both heat and momentum transfer to a parabolic dendritic interface which can be used to obtain growth rates and lengthscales. Then, Ananth and Gill (1988a,b, 1989) generalized Eq. 1 by considering the effect of an externally imposed flow of melt with velocity, U_{∞} , into which the dendrite propagates. They obtained moving boundary solutions to the Navier-Stokes and energy equations with the Oseen or Stokes flow approximation

Table 1. Growth Kinetics, V_G , R_1 , and R_2 , Reported by Various Investigators

Investigators	ΔT (K)	V_G (cm/s)	R_1 (μ m)	R_2 (μ m)	A
Kallungal (1977)	0.11–1.0	$0.0118\Delta T^{2.17}$	$\frac{0.6}{\Delta T}$	$\frac{43}{\Delta T^{1.24}}$	50–100
Fujioka (1978)	0.2–1.6	$0.0142\Delta T^{2.38}$			
Chang (1985)	0.2–1.0	$0.009\Delta T^{2.04}$		$\frac{39}{\Delta T^{1.1}}$	
Tirmizi (1985, 1987)	0.06–0.2	$0.0035\Delta T^{1.06}$			
	0.2–1.1	$0.0187\Delta T^{2.09}$	$\frac{0.88}{\Delta T}$		25–55
Present Work	0.035–1.000	$0.011\Delta T^{1.94}$	$\frac{1.51}{\Delta T}$	$\frac{42.0}{\Delta T}$	28

at low Reynolds numbers. Their result for the Stokes flow approximation is given by:

$$St = \frac{P_G}{2} \frac{2}{\int_1^{\infty} \exp \left[- \int_1^{\eta} f(\eta; Re, A, P_G, Pr) d\eta \right] d\eta} \quad (2)$$

where

$$f(\eta; Re, A, P_G, Pr) = 0.5 \left(P_G + \frac{1}{\eta} + \frac{1}{A-1+\eta} \right) - \frac{(\eta-1)}{\sqrt{\eta\{1+(\eta-1)/A\}}} \int_1^{\infty} \frac{\exp(-0.5Re_1\eta)}{\sqrt{\eta\{1+(\eta-1)/A\}}} d\eta + 2\sqrt{A} \ln \left(\frac{\sqrt{\eta} + \sqrt{A-1+\eta}}{1+\sqrt{A}} \right) \int_1^{\infty} \frac{\exp(-0.5Re_1\eta)}{\sqrt{\eta\{1+(\eta-1)/A\}}} d\eta$$

Here, $\eta = 1$ is the solid/liquid interface. The Reynolds numbers, $Re = U_{\infty} R_1 / \nu$ and $Re_1 = Re + V_G R_1 / \nu$, and the Prandtl number, $Pr = \nu / \alpha$, determine the importance of convection in the melt. Furthermore, Eq. 2 reduces to the heat conduction solution given by Eq. 1 as $Re \rightarrow 0$. We will compute additional results from Eq. 2 and compare them with our experiments.

For fixed ΔT , Eqs. 1 and 2 predict only a continuous family of P_G , the product of growth velocity and a lengthscale. The experiments, however, select unique values of V_G , R_1 and R_2 for the fully developed dendrite. Therefore, the ultimate theoretical problem is to predict these three characteristics, and it has been assumed to require such factors as anisotropy in the attachment kinetics and the interfacial tension in the theory. Attachment kinetics apparently limits growth normal to the basal plane. Its effect, however, may be negligible on the growth normal to the edge plane, which presumably is rough so that molecules experience little resistance in attaching themselves to the surface. Therefore, the propagation rate of a fully developed ice dendrite seems to be limited by the transport of heat which is driven by the difference in temperature between the interface, T_e , and the bulk of the melt, T_{∞} .

Capillarity due to interfacial tension lowers the interfacial temperature due to the curvature of the dendritic structure and is given by the Gibbs-Thomson equation,

$$T_e = T_m - \frac{T_m}{L} \left\{ \gamma(\theta, \phi)(\kappa_1 + \kappa_2) + \frac{\partial^2 \gamma}{\partial \theta^2} \kappa_1 + \frac{\partial^2 \gamma}{\partial \phi^2} \kappa_2 \right\} \quad (3)$$

where T_m is the normal freezing point of a planar interface, γ is the interfacial tension, θ and ϕ are the orientation angle with respect to the main axis of the dendrite, and κ_1 and κ_2 are local curvatures. At the tip of the dendrite, $\kappa_1 = 1/R_1$, and $\kappa_2 = 1/R_2$. The interfacial tension γ varies along the interface due to the crystalline anisotropy in molecular packing. Koo et al. (1991) determined the degree of anisotropy, ϵ , in the interfacial tension to be 0.002 and 0.3 along the basal and edge planes, respectively, by observing the equilibrium shape of the water droplets in ice matrix at the triple point temperature. For nearly isotropic material such as succinonitrile, Kessler et al. (1988) and Barbieri et al. (1986) considered fourfold anisotropy in the interfacial tension of a symmetric dendrite for which $R_1 = R_2 = R_m$ at the tip, and solved the conduction equations along with Eq. 3 for small values of ϵ , to arrive at,

$$\sigma^* = \frac{2\alpha d_0}{V_G R_m^2} = a \epsilon^{7/4} \quad (4)$$

where R_m is the mean radius of curvature at the tip, $d_0 = (T_m \gamma C_p)/L^2$ is the capillary length, a is a constant of order 1, and σ^* is the stability parameter. Equation 4, which is known as microscopic solvability, provides an independent relationship between V_G and R_m , which may be used in conjunction with Eq. 1 or 2 to determine V_G and R_m uniquely as independent functions of ΔT . There are several aspects to Eq. 4 that are still controversial.

Ananth and Gill (1988a, 1991) used $\sigma^* = 0.0195$ in Eq. 4 with Eq. 2 for $A = 1$ to account for the thermal convection effect and showed good agreement with the data on dendritic growth of succinonitrile from quiescent melt. They assumed that Eq. 4 is not affected much by thermal convection, which is accounted for through Eq. 2. Ice, however, is highly anisotropic with $R_2 > R_1$, and the radius of curvature at the tip is $R_m = 2R_1 R_2 / (R_1 + R_2)$. Therefore, we performed experiments to establish the stability parameter, σ^* .

During the dendritic growth of ice in quiescent pure water, thermal convection driven by gravity arises only in the neighborhood of the solid/liquid interface. Huang and Barduhn (1985) proposed a boundary layer theory for the natural convection governing the growth of a two-dimensional parabola. Their theory neglects the moving boundary effect and underpredicts the experimental results due to the two-dimensional idealization of the shape. No thermal convection theory exists for a three-dimensional moving elliptical paraboloid. Therefore, we relate the experiments of dendritic growth of ice to the results in Eq. 2, which describes forced convection through a thermal convection analogy, $Gr = Re_m^2$, $Re_m = (U_\infty R_m)/\nu$ and $Gr = (R_m^3 \beta g \Delta T)/\nu^2$ are the Reynolds and Grashof numbers, respectively. Gr represents the intensity of convection due to the thermal gradient created by the subcooling; g and β are the gravitational constant and coefficient of volumetric expansion of melt, respectively. The forced convection velocity, U_∞ , is taken to be equivalent to the characteristic thermal convection velocity of the fluid, $U_\infty = U_{nc} = \sqrt{\beta g \Delta T R_m}$. Ananth and Gill (1988b) showed that $Gr = Re^2$ is a good approximation by comparing succinonitrile experiments with their theoretical

model of a steady-state growth of the dendritic tips in the presence of thermal convection. Subsequently, Ananth and Gill (1989) applied their theory, which was driven by using the Oseen viscous flow approximation, to the dendritic growth of an ice crystal with forced convection. They showed that the effect of aspect ratio on the growth kinetics becomes less significant as the intensity of convection is increased, and their results agree qualitatively with the experiments of Kallungal and Barduhn (1977) and Chang (1985).

In our experiments, subcoolings as low as 0.035 K were employed. Therefore, it is crucial to have precise temperature control and high purity of water, which affect the freezing temperature. Also very accurate recording of the dendritic patterns is needed due to the very small lengthscales involved. In this article, we report new quantitative measurements of the growth kinetics and tip radii of ice dendrites at very small subcoolings of $0.035 \text{ K} < \Delta T < 1.000 \text{ K}$, where the natural convection plays a dominant role. The experimental results are compared with transport theories which are combined with the stability parameter.

Experimental Apparatus and Procedure

The experimental apparatus consists of a growth cell, thermistors for temperature measurement, a proportional temperature controller, a constant cooling and heating unit, and stirrers that are placed inside a constant temperature bath [3/8-in. (9.5-mm)-thick, 15-in. (381-mm) cube of plexiglass] containing ethylene glycol-water solution as the coolant. A microscope-camera (or VCR) assembly and light source are installed in line with the crystal growth cell for a direct, *in-situ* observation of the crystal growing freely in the growth cell. The cells used for upward and downward growth are similar to the one used by Glicksman et al. (1976) for succinonitrile experiments. They are made of Pyrex glass and are designed to ensure free growth of the ice crystal, as shown in Figure 1.

Nucleation is induced by liquid nitrogen, and the dendrite propagates along a capillary and emerges from the tip of the capillary to grow freely in subcooled water. In general, ice dendrites grow in arbitrary directions with respect to the observation system. Therefore, to investigate the effect of thermal (natural) convection induced by gravity on ice crystal growth and to photograph the edge and basal plane accurately, a system was designed that allows 360° rotation and $\pm 30^\circ$ tilting. This system enabled us to achieve any desired orientation as dendrites emerged from the capillary tip. In our experimental setup, potential sources of vibration such as the cooler and the stirrers are minimized by fixing the growth cell to the wall of the laboratory so that well-focused photographs can be taken without stopping the stirrers.

Control of the purity of the water used is very important because dissolved impurities in water lower the freezing point. Therefore, all parts of the crystal growth cell were cleaned with 10% hydrofluoric acid-water solution for 5 hours followed by immersion in distilled water for 24 hours. Finally, these cells were rinsed several times with HPLC-grade water.

We performed experiments using both water exposed to air (open system) and with water under vacuum (closed system). In the open cell, HPLC-grade water manufactured by Fisher Scientific Co. was used. The electrical resistivity of HPLC-grade water at 25°C was measured by using a digital multimeter

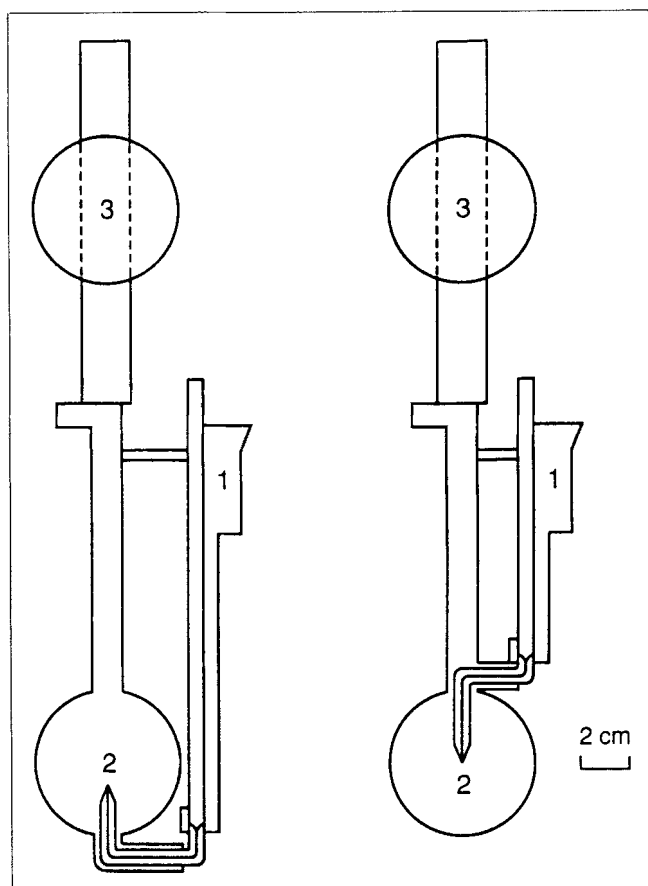


Figure 1. Growth cell: cells for upward (left) and downward (right) growth.

1. nucleation chamber; 2. crystal growth chamber; 3. rotating and tilting system.

(Model 8012A, Fluke Co.) and a digital electrometer (Model 616, Keithly Co.) and was found to be 1.8–2.1 $M\Omega \cdot cm$. In general, the resistivity of type-I deionized water (10–18 $M\Omega \cdot cm$ at 25°C) exposed to the open air rapidly decreases due primarily to the presence of CO_2 (typically 0.3–2 $M\Omega \cdot cm$). Therefore, most of the impurity in our water seems to be dissolved air. The purity level of the water in our open system was calculated by following the procedure described by Schooley et al. (1986) and was found to be approximately 99.99%. To maintain the purity of water during the experiments, the water in the growth cell is replaced and the cell is cleaned periodically with acetone.

The effect of dissolved air on dendritic growth was studied by sealing the growth cell hermetically with air-free pure water using the vacuum distillation followed by several melting and freezing steps to expel most of dissolved air. The level of the purity of the water in the closed growth cell was determined by measuring the triple point. Vacuum distillation and alternate melting and freezing were used to fill the triple-point cell with pure water using the procedure that is similar to that adopted for the growth cell. The triple points of our cell and the master cell, which was manufactured by Jarrett Instrument Co., were measured using the sheath method described by Cox and Vaughan (1982) and Ferguson (1970). The difference in triple points between both cells is found to be within 0.5 mK. Thus, the purity level of water we used under vacuum in our closed

cell was estimated to be better than 99.999%, which was an order of magnitude better than that in our open cell.

Temperature measurement and control

To measure the temperature of the constant temperature bath, a precision thermistor (Model S-25, Serial Number 329, Thermometric Inc.) calibrated by the National Institute of Standards and Technology is located just beside the crystal growth chamber. Recalibration was carried out in our laboratory by using the water and succinonitrile triple point cells. The electrical resistance of the thermistor is measured indirectly with a digital nanovoltmeter (Model 181, Keithly Instruments, Inc.). The voltage is read when a steady current is passed through the thermistor from the constant current source (Model CS-1000B, Cryocal Inc.). The voltage measured by this procedure can be converted to resistance, and thus the bath temperature can be determined precisely by using a calibration table of resistance and temperature. The temperature of the bath is controlled by a precision temperature controller (Model 123, Bayley Instrument Co.) and a portable cooling unit (Model PCC-13A-3, Blue M Electric Co.). The temperature of the ethylene glycol solution in the constant temperature bath is controlled very carefully by using a cooling unit and a 100-W electric immersion heater with quartz sheath. An additional amount of heat, proportional to the difference between the bath temperature and the set point, is provided by an electric heater (500-W, stainless-steel immersion heater), which is plugged into the controller. With these control assemblies, vigorous stirring, and proper insulation, the bath temperature was recorded to be stable to ± 0.002 K for over 10 hours.

Photography and video recording

Pictures of the growing crystals were recorded by using a microscope-video camera (Digital 500CCD, Panasonic Inc.) with a video cassette recorder (VO-9600, Sony Inc.) and a frame code generator (FCG 700, Sony Inc.) or were photographed on 35-mm Ilford (ASA 400) films with a 35-mm camera (Model Wild M 420, Ernst Leitz Inc.). The microscope is mounted on an X-Y axis unislide (Vermax, Inc.), which can be easily moved to follow the crystal tip during its growth. The position of the light source was also controlled to track the crystal using a unislide (Model E-552-M, Electrol Craft Co.). To minimize the optical distortion caused by the difference of the refractive index between pure water in the growth cell and the coolant, 7.5 vol. % ethylene glycol solution was used. The freezing point of the solution is about $-3^\circ C$, and the difference in the refractive indices was measured to be about 0.004 at $27^\circ C$. Thus, the optical distortion between these two media is negligible.

Experimental procedure

The effect of the natural convection induced by gravity on ice crystal growth was studied by adjusting the cell such that the ice dendrites grow upward or downward parallel to gravity vector, g , and lie in the plane of observation so that the photographs are not distorted.

To calculate the growth velocity of the ice dendrite as a function of time, the distance traveled by the dendritic tip is measured by using a reticle inserted in the eye piece of the

microscope. The time elapsed is measured with a stop watch. The capillary of the growth cell and a scientific scale (American Optics Co.) were used to calculate the magnification of the microscope. Negative films were used to calculate the tip radius of the edge and basal planes as a function of time. The negative film is mounted on the transverse stage of Microcalc-1 (RAM Optical Instrument Co.), in which the magnified image of the dendrite is transmitted to the screen of the monitor that has an X-Y axis, via a microscope-CCD solid-state camera system. The width w of the crystal at a distance l from the tip of the crystal can be measured with a resolution of $1\text{ }\mu\text{m}$ by moving the transverse stage. Assuming that the shape of the image of dendrites is parabolic, the tip radius can be calculated by the formula $R = w^2/8l$. The error in the growth velocity, V_G , and tip radii, R_1 and R_2 , were within $\pm 5\%$, $\pm 10\%$, respectively.

Experimental Results and Discussion

From the phase diagram, one can expect a difference in freezing point of about 0.01 K between highly pure (99.99%) and ultra pure (99.999%) water. The effect of dissolved air on the dendritic growth kinetics of ice, however, was found to be negligible for subcoolings greater than 0.06 K .

Figures 2A and 2B show the basal plane and the edge plane of a typical ice dendrite. The tip radius of the edge plane, R_1 , is much smaller than that of the basal plane, R_2 . Figure 3A shows the velocity of ice dendrites growing vertically upward measured with time. Time $t=0$ represents the point where the crystal emerges from the capillary tip. Figure 3A shows that, at $\Delta T > 0.1\text{ K}$, a steady growth velocity developed as soon as the ice crystal emerged from the capillary tip. At $\Delta T < 0.1\text{ K}$, however, a steady state is reached only after an initial transient state that lasts longer as the subcooling decreases. This observation is consistent with previous experiments of ice crystals. Fujioka (1978) observed that the growth velocity of submerged ice disk decreases at small subcoolings, and Chang (1985) also pointed out this fact. The growth velocity in the transient state also is found to be higher in other materials such as krypton

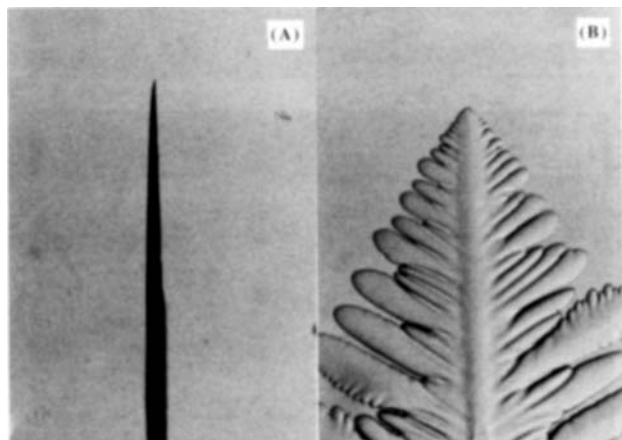


Figure 2. Typical morphology of the ice dendrite; (A) edge view; (B) basal view.

Subcooling, 0.607 K ; magnification, $26\times$.

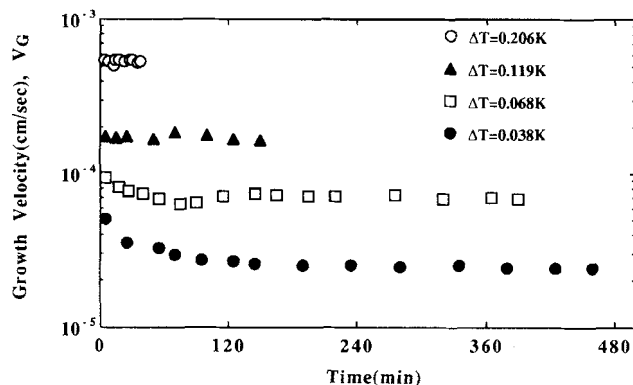


Figure 3A. Growth velocity of ice dendrites with time: vertically upward growth.

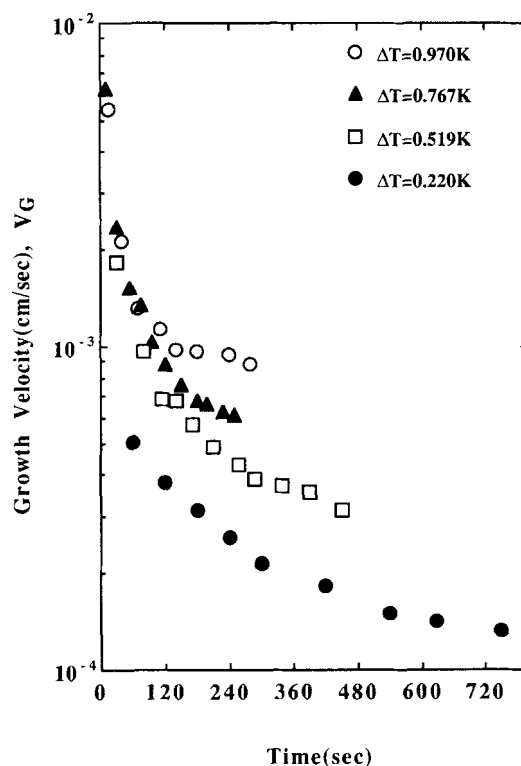


Figure 3B. Growth velocity of ice dendrites with time: vertically downward growth.

(1988). In the transient state, the growth pattern of ice crystal evolves with time, namely, from a disk to a dendrite.

Figure 3B shows the velocity of dendrites growing downward, and clearly no steady state was observed. This is because gravity induces warmer fluid to flow down the side of the crystal toward the tip, which retards growth, and the tip size increases with time. At a very large subcooling, natural convection is negligible at steady state. Therefore, dendrites growing vertically downward also can reach a steady state. The slope with time of the growth velocity of dendrites growing downward, however, decreases faster as subcooling increases, as can be seen in Figure 3B. Consequently, the radius of the curvature increases with time, and the slope at high subcoolings is larger than that at small subcoolings. Figure 4 illustrates the

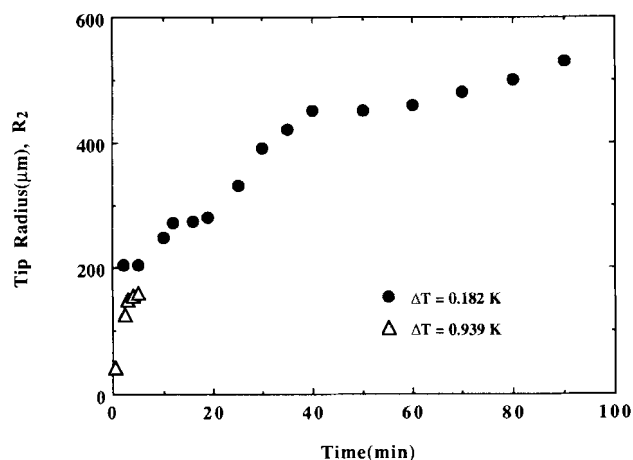


Figure 4. Change of the radius of basal plane with time for dendrite growing vertically downward.

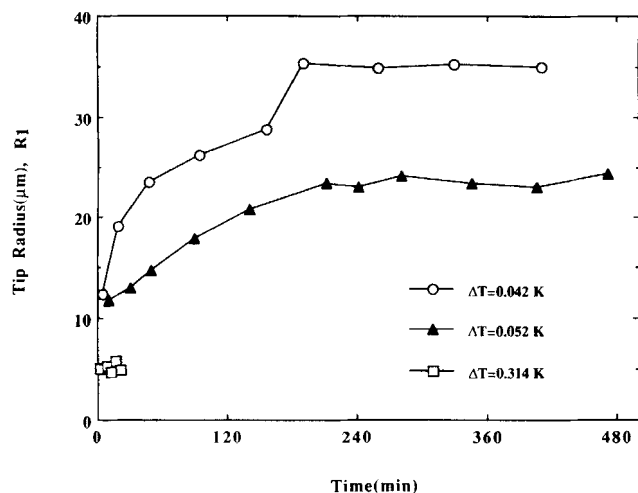


Figure 5A. Tip radius measured with time for dendrite growing vertically upward: edge plane, R_1 .

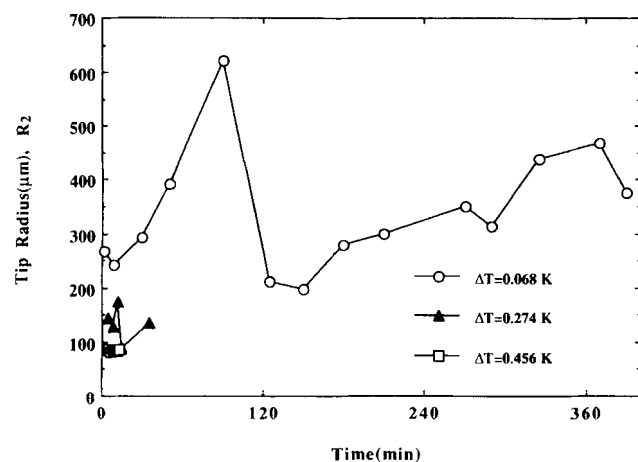


Figure 5B. Tip radius measured with time for dendrite growing vertically upward: basal plane, R_2 .

change of tip size of the basal plane with time. Clearly, at $\Delta T = 0.939$ K, the size of R_2 rapidly increased, while at $\Delta T = 0.182$ K, the size of the tip slowly increased. It seems, therefore, that a dendrite growing downward is affected by thermal convection from the whole dendrite unlike the case of a dendrite growing vertically upward.

Figure 5A illustrates that R_1 has an initial transient state at $\Delta T < 0.1$ K, as does the growth velocity, after which R_1 reaches a steady-state value for a fixed subcooling ΔT . The time period of the initial transient in R_1 is approximately the same as that of the initial transient of the growth velocity at given subcoolings. On the other hand, the tip of the basal plane changes continuously due to the tip splitting events that occur at $\Delta T < 0.35$ K, as shown in Figure 5B. The tip splitting phenomenon of the ice dendrite has been discussed in detail by Koo et al. (1991) recently. Their photographs show clearly that the tip of the basal plane increases in size until the tip becomes morphologically unstable and splits, often unsymmetrically. In general, the tip splits into two which compete with each other until one of them becomes the leading tip and the other becomes a side branch with respect to the main axis. Therefore, the size of R_2 drops upon splitting, and the R_2 of the leading tip then increases in size as time progresses until it undergoes another tip splitting event. Tip splitting in the basal plane occurs repeatedly, and R_2 does not appear to approach a steady value unlike the growth rate V_G and R_1 for subcoolings less than 0.35 K. At larger subcoolings the tip propagates steadily with a constant R_2 for fixed ΔT , and no tip splitting event was

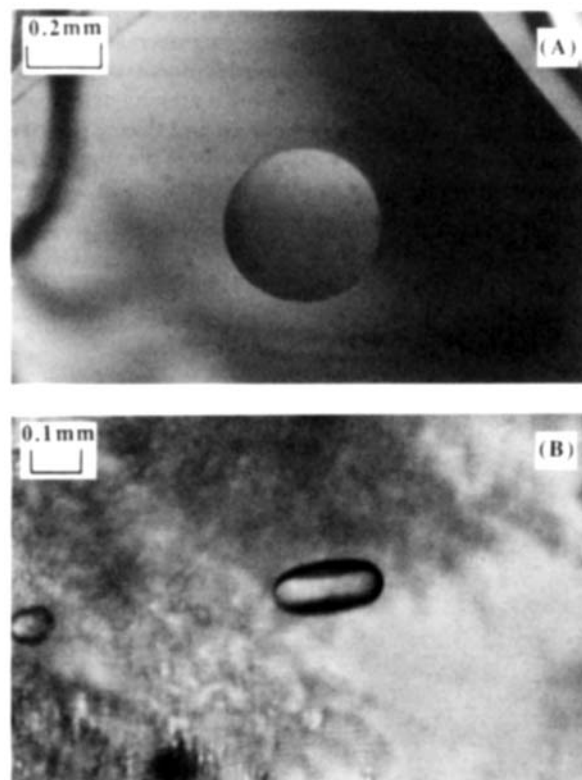


Figure 6. Equilibrium shape of water droplet in ice matrix: (A) basal plane; (B) edge plane.

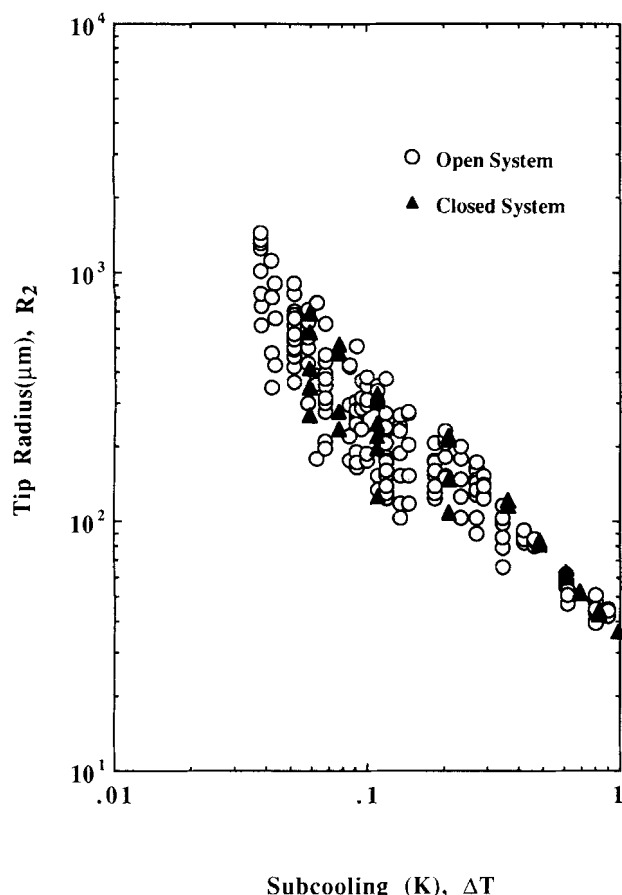


Figure 7. Tip radius of the basal plane, R_2 , vs. subcooling.

observed. In the light of microscopic solvability theory of dendritic growth, it seems that the tip splitting phenomenon may be caused by the lack of anisotropy in the interfacial tension, which destabilized the interface against morphological perturbations along the basal plane. Koo et al. (1991) reported the degree of anisotropy, ϵ_6 , in the basal plane to be very small (less than 0.002) and, ϵ_2 , in the edge plane to be 0.3 by measuring the deviation in the shape of the equilibrium droplet of water from a perfect sphere. The typical shape of a water droplet in an ice matrix is shown in Figure 6. Furthermore, the fluid velocity due to the thermal convection becomes bigger than the growth velocity of the ice dendrite at $\Delta T < 0.35^\circ\text{C}$ and may contribute to the destabilization of the solid/liquid interface.

Even though the radius of the curvature of the basal plane

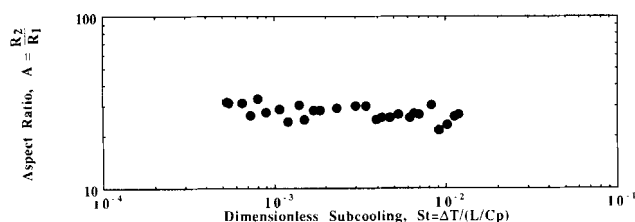


Figure 8. Aspect ratio, A , vs. dimensionless subcooling, St .

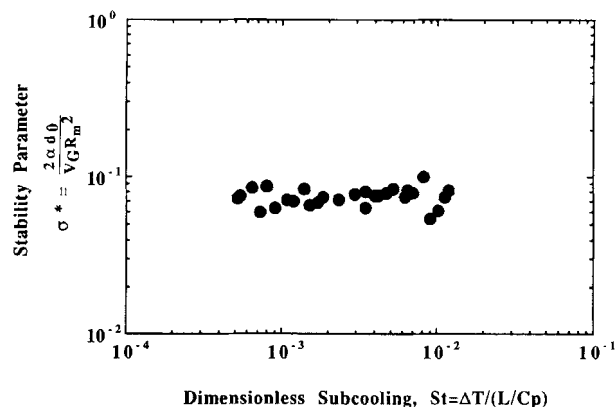


Figure 9. Stability parameter, σ^* , vs. dimensionless subcooling, St .

changes with time, there seems to exist a unique maximum value for R_2 which is reproducible at a fixed subcooling, as shown in Figure 7. For a given subcooling, a range of values for R_2 is shown in Figure 7, since R_2 changes with time at $\Delta T < 0.35\text{ K}$. The maximum values for R_2 are approximately proportional to the inverse of the subcooling, as shown in Table 1. Table 1 also shows power law correlations of our data for V_G and R_1 with the subcooling. Figure 8 shows that the aspect ratio $A = R_2/R_1$ remains independent of dimensionless subcooling and that of the tip of the ice dendrite is about 28 over the entire range of the present experiments. Thus, using an elliptical paraboloid as an approximation for the shape of the tip of ice crystal seems to be reasonable. For $\Delta T < 0.35\text{ K}$, where tip splitting occurred, the maximum value for R_2 has been used in calculating the aspect ratio. Next, we will compare the experimental data for the growth rate V_G , and tip radii, R_1 and R_2 , as a function of ΔT , with theoretical models, which consider the fully three-dimensional elliptical paraboloid shape and therefore contain the aspect ratio, $A = R_2/R_1$, as a parameter.

Figure 9 shows that the stability parameter for ice dendrites, as given by Eq. 4 with $R_m = 2R_1R_2/(R_1 + R_2)$, is $\sigma^* = 0.075$ and

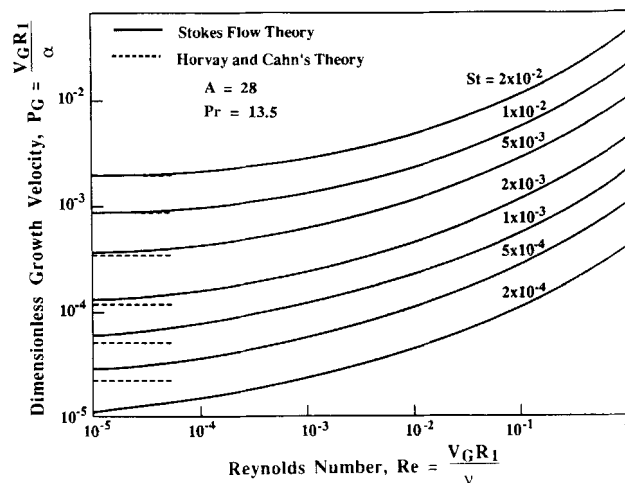


Figure 10. Growth Peclet number, P_G , predicted by Stokes flow theory as a function of Reynolds number.

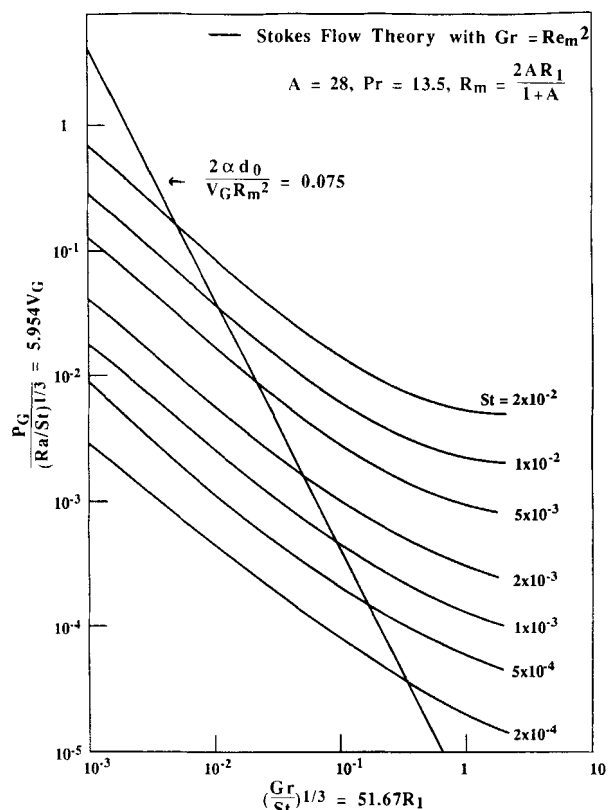


Figure 11. Operating point predicted by Stokes flow theory with the stability parameter.

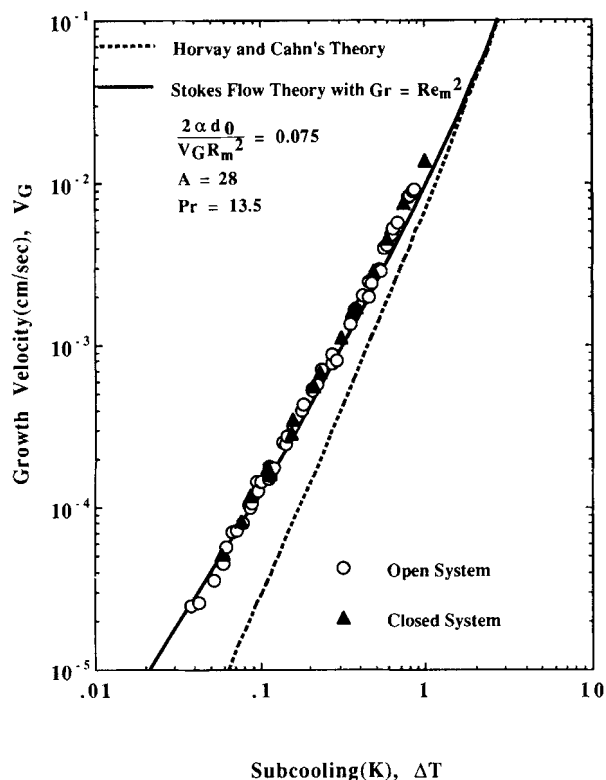


Figure 12. Comparison of growth velocity, V_G , with the prediction of theories.

is independent of the subcooling over the entire range of the experimental data. Below $\Delta T = 0.35$ K, the maximum values of R_2 were selected, since R_2 depends on time due to tip splitting. Figure 10 shows the theoretical predictions for the growth Peclet number for both Eqs. 1 and 2. Clearly, as the intensity of convection in the melt Re increases, P_G increases from its pure conduction values, which are shown by the broken lines. Furthermore, the effect of convection is more important at small subcoolings as indicated by larger difference between the conduction and convection theories as St decreases. This is because the effect of the moving boundary dominates at larger St due to large growth rates. Indeed, in our experiments, as the subcooling decreases it is observed that the growth Peclet number becomes increasingly higher than that predicted by Eq. 1. Similar behavior was observed in succinonitrile and pivalic acid experiments by Huang and Glicksman (1981) and Glicksman (1984). Next, we will show that this is due to thermal convection in the melt, which enhances the heat removal from the interface, by following the methodology used by Ananth and Gill (1989) in explaining the data for dendritic growth of succinonitrile.

The Reynolds number in Figure 10 represents the intensity of forced convection and it may be related approximately to Grashof number by $Gr = Re_m^2$, where Gr represents the intensity of thermal convection in our experiment. Thus, P_G , for fixed Gr and St , can be obtained from Figure 10 by using the thermal convection analogy. We then can calculate the dimensionless group $P_G / (Ra/St)^{1/3}$ and $(Gr/St)^{1/3}$, at given subcooling, which represent the growth velocity and lengthscale, respectively. By substituting the definition for P_G , Ra , Gr , and St , one gets $P_G / (Ra/St)^{1/3} = 5.954 V_G$ and $(Gr/St)^{1/3} = 51.67 R_1$, respectively.

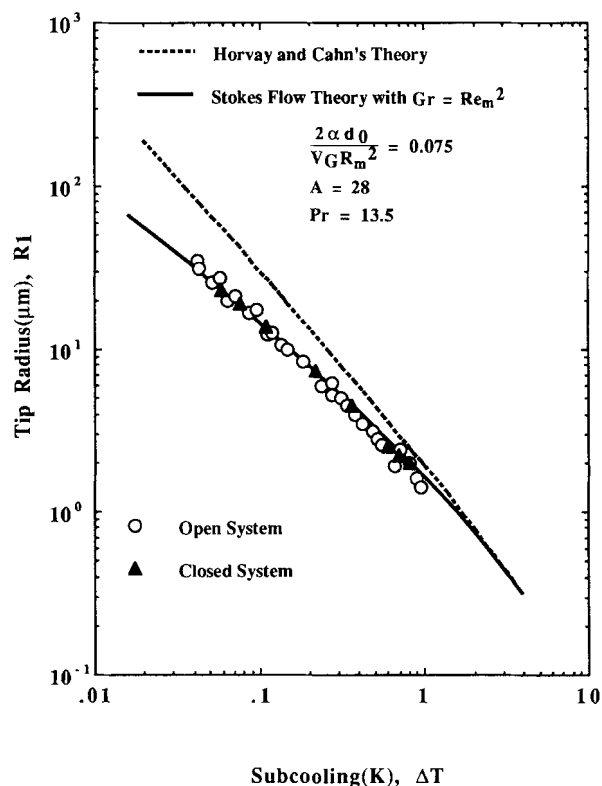


Figure 13. Comparison of tip radius of the edge plane, R_1 , with the prediction of theories.

In this way, Figure 11 shows the predicted values of V_G as a function of R_1 and St in dimensionless form. Figure 11, which includes the stability relationship $(2\alpha d_0)/V_G R_m^2 = 0.075$, gives the operating point for a given subcooling. The intersection of the straight line and the curves in Figure 11 yields unique growth velocity and lengthscale at a given subcooling. The relationships for V_G and R_1 as functions of subcooling are shown in Figures 12 and 13.

Figures 12–14 show that the theory of Horvay and Cahn combined with the stability parameter predicts growth velocities and tip radii, which differ significantly from our experimental data. When convection is included in the theory, however, agreement with the present experiments is good. Figure 15 shows reasonable agreement between the experiments and the prediction for the Grashof number and that the lengthscale of ice dendrites is the harmonic average of tip radii, R_1 and R_2 , rather than the radius of curvature of the edge plane, R_1 , which previously has been used as the lengthscale. All data used in this article were tabulated by Koo (1991).

Conclusions

Our experiments show that natural convection, as indicated by the Grashof number, becomes the dominant mode of heat transfer at the solid/liquid interface as the subcooling decreases ($\Delta T < 0.35$ K). As a result, the observed growth velocity of ice is higher than that predicted by Horvay and Cahn's pure conduction theory of an elliptical paraboloid. Thus, the present experimental results corroborate qualitatively the thermal convection theory of Ananth and Gill (1988) for a paraboloid of revolution.

The experimental data also show that ice dendrites have an aspect ratio $A = 28$, and the stability constant based on Eq. 4 is 0.075. The values of V_G , R_1 and R_2 , predicted by the moving boundary solutions of the Navier-Stokes and energy equations agree well with the present experiments when one uses the

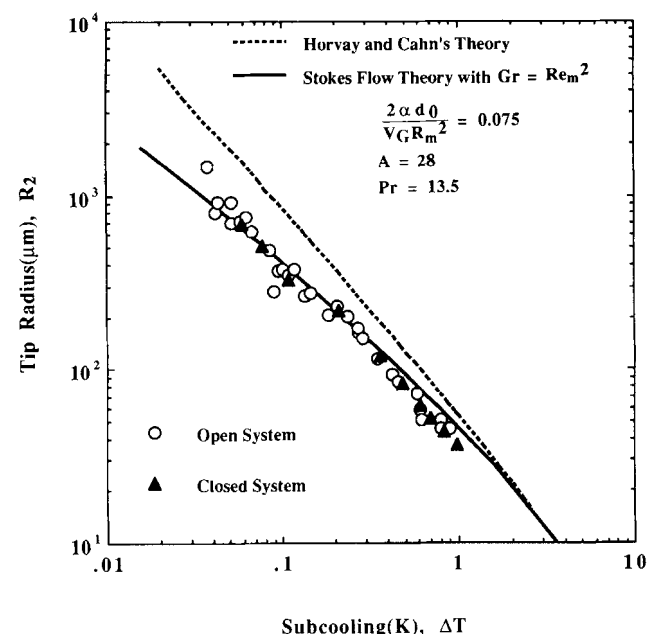


Figure 14. Comparison of tip radius of the basal plane, R_2 , with the prediction of theories.

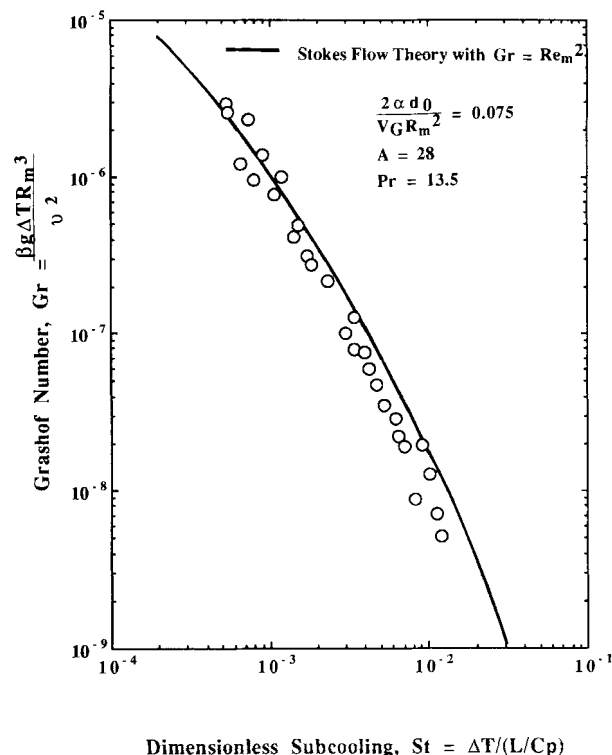


Figure 15. Comparison of Grashof number between experiments and predicted by Stokes flow theory with the thermal convection analogy.

thermal convection analogy and $\sigma^* = 0.075$. In contrast, the conduction theory of Horvay and Cahn, which neglects convection as well as the stability parameter, deviates significantly from the experimental data.

By using the thermal convection analogy and the experiments, it was found that the lengthscale for dendrites of ice crystals is the harmonic mean of the tip radii of the edge and basal planes, $(2R_1R_2)/(R_1 + R_2)$, rather than the radius of the edge plane, R_1 .

Acknowledgment

This work was supported in part by NSF and the New York State Energy Research and Development Authority.

Notation

- A = aspect ratio of the dendrite tip of the ice crystal, R_1/R_2
- C_p = heat capacity of melt
- d_0 = capillary length, $(T_m\gamma C_p)/L^2$
- g = acceleration due to gravity
- Gr = Grashof number, $(g\beta\Delta TR_m^3)/\nu^2$
- L = latent heat
- P_G = growth Peclet number, $(V_G R_1)/\nu$
- Pr = Prandtl number, ν/α
- R_1 = tip radius of the edge plane
- R_2 = tip radius of the basal plane
- R_m = the harmonic mean of the tip radii, $(2R_1R_2)/(R_1 + R_2)$
- Ra = Rayleigh number, $GrPr$
- Re = Reynolds number, $(U_\infty R_1)/\nu$
- Re_1 = combined Reynolds number, $Re + [(V_G R_1)/\nu]$
- Re_m = Reynolds number, $(U_\infty R_m)/\nu$
- St = Stefan number, $\Delta T/(L/C_p)$
- T_m = normal freezing temperature

T_{∞} = subcooled temperature of the melt
 ΔT = subcooling, $T_m - T_{\infty}$
 U_{∞} = forced convection velocity
 V_G = growth velocity of dendrite

Greek letters

α = thermal diffusivity of the melt
 β = thermal expansion coefficient

$$= \frac{1}{\rho_{\infty}} \left(\frac{\partial \rho}{\partial T} \right)$$

 γ = surface tension
 ϵ = degree of anisotropy in surface tension
 σ^* = morphological stability parameter, $(2\alpha d_0)/(V_G R_m^2)$
 ν = kinematic viscosity of the melt

Literature Cited

- Ananth, R., and W. N. Gill, "Dendritic Growth with Thermal Convection," *J. of Crystal Growth*, **91**, 587 (1988a).
 Ananth, R., and W. N. Gill, "The Effect of Convection on Axisymmetric Parabolic Dendrites," *Chem. Eng. Commun.*, **68**, 1 (1988b).
 Ananth, R., and W. N. Gill, "Dendritic Growth of An Elliptical Paraboloid with Forced Convection," *J. Fluid Mech.*, **208**, 575 (1989).
 Ananth, R., and W. N. Gill, "Self-Consistent Theory of Dendritic Growth with Convection," *J. of Crystal Growth*, **108**, 173 (1991).
 Barbieri, A., D. C. Hong, and J. S. Langer, "Velocity Selection in The Symmetric Model of Dendritic Crystal Growth," *Phys. Rev. A*, **35**, 1802 (1987).
 Bilgram, J. H., M. Firmann, and W. Kanzig, "Dendritic Solidification of Krypton and Xenon," *Phys. Rev. B*, **37**, 685 (1988).
 Chang, L. Y., "Dynamic and Steady-State Process of Crystal Growth in Quiescent and Flow Systems," PhD Diss., State Univ. of New York at Buffalo (1985).
 Cox, J. D., and M. E. Vaughan, *Temperature, Its Measurement and Control in Science and Industry*, p. 267, J. F. Schooley, ed., AIP, New York (1982).
 Dash, S., and W. N. Gill, "Forced Convection Heat and Momentum Transfer to Dendritic Structures (Parabolic Cylinders and Paraboloids of Revolution)," *Int. J. Heat Mass Transfer*, **27**, 1345 (1984).
 Ferguson, J. A., "Realization of the Triple Point of Water," *J. Physics E.*, **3**, 447 (1970).
 Fujioka, T., "Study of Ice Growth in Slightly Undercooled Water," PhD Diss., Carnegie-Mellon University, Pittsburgh, Pennsylvania (1978).
 Gill, W. N., "Heat Transfer in Crystal Growth Dynamics," *Chem. Eng. Prog.*, **85**, 33 (1989).
 Glicksman, M. E., R. J. Schaefer, and J. D. Ayers, "Dendritic Growth—a Test of Theory," *Met. Trans. A.*, **7A**, 1747 (1976).
 Glicksman, M. E., "Free Dendritic Growth," *Mat. Sci. Eng.*, **65**, 45 (1984).
 Glicksman, M. E., E. Winsa, R. C. Hahn, T. A. Lograsso, S. H. Tirmizi, and M. E. Selleck, "Isothermal Dendritic Growth—A Proposed Microgravity Experiments," *Metall. Trans. A*, **19A**, 1945 (1988).
 Horvay, G., and J. W. Cahn, "Dendrite and Spherical Growth," *Acta Metall.*, **9**, 695 (1961).
 Huang, J. S., and A. J. Barduhn, "The Effect of Natural Convection on Ice Crystal Growth Rates in Salt Solutions," *AIChE J.*, **31**, 747 (1985).
 Huang, S. C., and M. E. Glicksman, "Fundamentals of Dendritic Solidification: I. Steady-State Tip Growth," *Acta Metall.*, **29**, 701 (1981).
 Ivantsov, G. P., "Temperature Field Around Spherical, Cylindrical and Needle-Shaped Crystals Which Grow in Supercooled Melt," *Dokl. Akad. Nauk. USSR*, **58**, 567 (1947).
 Kallungal, J. P., and A. J. Barduhn, "Growth Rates of An Ice Crystal in Subcooled Pure Water," *AIChE J.*, **23**(3), 294 (1977).
 Kessler, D., J. Koplik, and H. Levine, "Steady State Dendritic Crystal Growth," *Phys. Rev. A*, **33**, 3352 (1986).
 Kessler, D., J. Koplik, and H. Levine, "Pattern Selection in Fingered Growth Phenomena," *Adv. in Phys.*, **37**, 255 (1988).
 Kind, M., W. N. Gill, and R. Ananth, "The Growth of Ice Dendrites Under Mixed Convection Conditions," *Chem. Eng. Comm.*, **55**, 295 (1987).
 Koo, K.-K., "Dendritic Growth of Ice Crystals with Natural Convection," PhD Diss., Rensselaer Polytechnic Institute, Troy, NY (1991).
 Koo, K.-K., R. Ananth, and W. N. Gill, "Tip Splitting in Dendritic Growth of Ice Crystals," *Phys. Rev. A*, **44**, 3782 (1991).
 Schooley, J. F., *Thermometry*, p. 33, CRC Press Inc., Boca Raton, FL (1986).
 Tirmizi, S. H., and W. N. Gill, "Effect of Natural Convection on Growth Velocity and Morphology of Dendritic Ice Crystals," *J. Crystal Growth*, **85**, 488 (1987).
 Tirmizi, S. H., and W. N. Gill, "Experimental Investigation of the Dynamics of Spontaneous Pattern Formation During Dendritic Ice Crystal Growth," *J. Crystal Growth*, **96**, 277 (1989).

Manuscript received Dec. 6, 1991, and revision received Apr. 15, 1992.